

Modelling of Helical Gearing with Machining Errors for Load Calculation

A. H. Elkholy and M. A. Alfares
Mechanical and Industrial Engineering Department
Kuwait University
P.O. Box: 5969, Safat, 13060
Kuwait

Fax: +965-4847131 – Email: kholy@kuc01.kuniv.edu.kw – www.eng.kuniv.edu.kw

Abstract

A procedure for calculating load distribution on oblique contact lines of helical gear teeth is introduced. The effect of both machining errors and profile modification is accounted for. The procedure is based upon stiffness calculation and assumes that the sum of tooth deflection, profile modification and machining errors at the pairs of contacting teeth are all equal. It is also assumed that the sum of the normal loads contributed by each pair of contracting teeth is equal to the total normal load. A detailed case study is outlined to explain the procedure. Experimental substantiation to prove the validity of the procedure is also introduced, where tooth fillet stresses were measured using strain gauges and the results were compared with those obtained from the procedure.

Keywords: Helical gears, tooth stiffness, profile modification, machining error

Nomenclature

a, b, ℓ	= gear geometry from Figure (4)
E	= Young's modulus of elasticity
EL	= lead error
F_1, F_2, \dots, F_m	= individual tooth loads
F_{ije}	= normal loads from segment j at tooth i
F_m	= total normal force transmitted by all meshing teeth
K_{ij}, K_{ij}^*	= segment stiffness of driver and driven gears, respectively
K_{ije}	= equivalent (combined) stiffness of driver and driven gear segments
PV	= profile deviation
s_1, s_2, \dots, s_6	= segment widths as per Figure (4)
SE	= spacing error
TD	= total displacement
α	= profile modification
ΔF	= segment normal load
$\Delta \delta$	= segment total deflection
ω	= angle between contact line and helix tangent
ψ	= helix angle
ϕ_t	= transverse pressure angle

1 Introduction

In the meshing of helical gears, which are used to eliminate the abrupt change of tooth stiffness in spur gears, the contact line of a pair of mating teeth moves towards the gear axis, varying the combined stiffness of the teeth. It is important to know the stiffness variation in order to determine load distribution along contact lines. It was found by Neriya et al [1] and Litvin et al [2] that tooth stiffness, in general, governs the mal-distribution of load arising from tooth deflection. Profile modification and machining errors play an important roll in determining the final load distribution and sharing among meshing teeth, as well.

Exact determination of load distribution along meshing teeth enables gear designers to establish fillet and contact stresses with gears under investigation. Consequently, areas of maximum stresses where failures may occur due to tooth breakages, excessive pitting or spalling may thus be found. Load distribution and sharing together with the study of gear kinematics help in the study of flash temperature distribution along contact lines and consequently the determination of the probability of gear failure due to scuffing.

In this study, a closed form procedure for calculating load distribution and sharing among helical gear teeth is introduced. The procedure is based upon determining tooth stiffness variation along contact lines; and utilizing the experience already gained in spur gear analysis to find load distribution.

2 Tooth Modelling And Deflection

Each tooth of the gear was modelled as a series of equal width segments, as shown in Figure (1). Each segment was then approximated as a spur gear of a finite face width, whose force-deflection relationship is determined from Nakada and Utagawa [3] and can be expressed as:

$$\Delta F = \Delta \delta . K \quad (1)$$

where $\Delta \delta$ is the segment deflection due to the application of ΔF load, and K is the segment stiffness which depends on its geometry and point of load application along the involute profile as outlined in Kasuba and Evans [4]. Obviously, the higher the number of these segments, the thinner their face widths become, and the more representative the modeling of the entire helical gear as a series of segmental spur gears becomes. Under the assumption of mathematically exact geometry, the teeth are in perfect contact even when unloaded. Under load application, however, each segment of a gear in the multiple contact zone will experience the same deflection as the corresponding segment on the mating gear, when these two segments come in contact. This condition is necessary to maintain contact and avoid interference,

Elkholy [5]. This suggests that load sharing among meshing segments on mating teeth should be in such a way to produce same deflection in these segments.

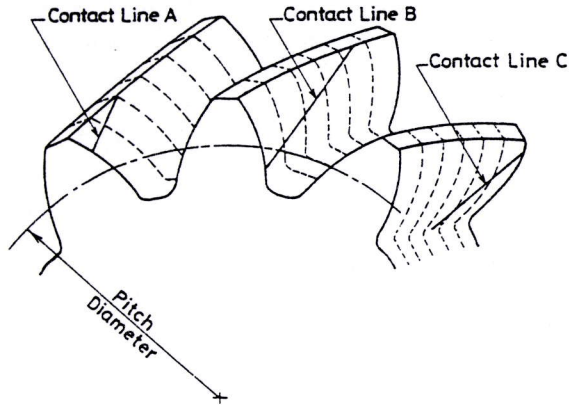


Figure (1) Tooth Modelling as a Series of Equal Width Segments.

Due to the inherent flexibility of the meshing gear teeth, they deflect from their true position and the deflection must be the same for each pair of teeth in the region of multiple pair contact. Following a similar argument, segments on the same line of contact should experience equal deflection in order to maintain contact between meshing teeth, Vijayakar et al [6].

In short, if a total external normal force F_m ($F_m = \text{Applied torque}/\text{base radius}$) is applied on a pair of helical gears, it will be distributed along lines of contact on meshing teeth according to the following two conditions:

- (1) Combined deflections of meshing teeth on different tooth pairs should be identical.
- (2) Combined deflections along contact lines on loaded teeth should be constant.

These two conditions are the basis for calculating load distribution and sharing in helical gear teeth.

3 Stiffness and Load Calculation

The stiffness of each segment of meshing teeth shown in Figure (1) is defined as the normal force applied to the segment to produce a unit deflection in the normal direction. Each segment may thus be modelled by a spring whose stiffness equals the segment stiffness. The number of segments forming one tooth on one gear is thus modelled as a series of springs connected in parallel; since they experience equal deflections under a given load. The segments on other meshing teeth of the same gear are also modelled as springs connected in parallel (equal deflection case as well).

Same procedure was followed for the segments of the mating gear. However, a segment on one gear (say the driver) and another meshing segment on the mating gear (the driven) should be represented by two springs connected in series since they experience the same applied load. Figure (2) outlines the stiffness modelling of the entire meshing teeth of both the driver and driven gears. It is assumed that we have m teeth in multiple contact of the driver and driven. Each tooth is divided into a finite number of segments i, j, \dots, k on tooth $1, 2, \dots, m$ as shown in the figure. Segment stiffnesses of the driver are given the symbol K_{mk} whereas that of the driven are given the symbol K_{mk}^* . Segment stiffnesses at each tooth in contact on the driver are combined with their corresponding segments of the mating tooth on the driven gear.

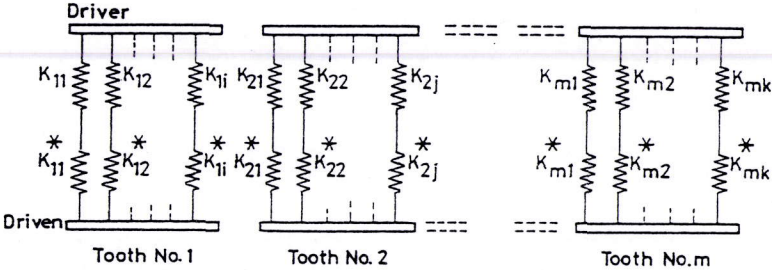


Figure (2) Stiffness Layout

The net stiffnesses of the segments are shown in Figure (3) where the individual tooth loads are F_1, F_2, \dots, F_m as given in the figure. The total normal load F_m becomes,

$$F_m = F_1 + F_2 + \dots + F_m \tag{2}$$

and the fraction load of each segment can thus be found from the tooth loads and net stiffnesses as:

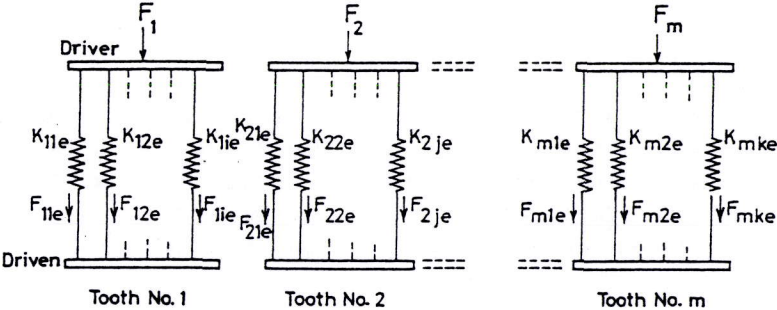


Figure (3) Combined Stiffness of Driver and Driven Segments

$$\begin{aligned}
F_{11e} &= F_1 \frac{K_{11e}}{\sum K_1} & F_{12e} &= F_1 \frac{K_{12e}}{\sum K_1} \dots & F_{1ie} &= F_1 \frac{K_{1ie}}{\sum K_1} \\
F_{21e} &= F_2 \frac{K_{21e}}{\sum K_2} & F_{22e} &= F_2 \frac{K_{22e}}{\sum K_2} \dots & F_{2je} &= F_2 \frac{K_{2je}}{\sum K_2} \\
\dots & & & & & \\
F_{m1e} &= F_m \frac{K_{m1e}}{\sum K_m} & F_{m2e} &= F_m \frac{K_{m2e}}{\sum K_m} \dots & F_{mke} &= F_m \frac{K_{mke}}{\sum K_m}
\end{aligned} \tag{3}$$

where

$$\begin{aligned}
\sum K_1 &= K_{11e} + K_{12e} + \dots K_{1ie} & i &= 1, 2, 3, \dots \\
\sum K_2 &= K_{21e} + K_{22e} + \dots K_{2je} & j &= 1, 2, 3, \dots \\
\dots & & & \dots \\
\sum K_m &= K_{m1e} + K_{m2e} + \dots K_{mke} & k &= 1, 2, 3, \dots
\end{aligned}$$

Equations (2) and (3) represents $(i+j+\dots k)m$ equations in same number of unknowns. Solving these equations determines individual segment loads for all teeth in contact and consequently tooth load distribution along lines of contact as well as load sharing among meshing teeth.

4 Profile Deviation Effect

There are cases when tooth flank geometry no longer follows the elementary pattern described by simple combination of the line elements of involute and helix. There are many reasons behind these deviations which are summarized by Ueno et al [7] and attributed to:

- (a) Profile modification like tip relief and/or root relief
- (b) Spacing error
- (c) Lead error
- (d) Shaft twist and bending

When such deviations are introduced to the analysis, tooth segment deflections along lines of contact are no longer equal; and deflections of meshing teeth are also different. Profile deviations PV should be accounted for as follows: total displacements TD (rather than deflections) of the segments on the same tooth must be equal. Total displacement is defined as the sum of segment deflection and profile deviation:

$$TD = \Delta\delta + PV \tag{4}$$

The profile deviation term PV may include one, or more, factors of those mentioned above. Similarly, total displacements of the teeth in mesh at the given instant of time, must be equal, and an equation like (4) should also be used.

The model in this study permits the investigation of more than one deviation at the same time. This is done, simply, by altering the term PV in equation (4) to allow for as many deviations as required. In other words:

$$\begin{aligned}
 TD &= \Delta\delta + \alpha \pm SE && \text{for mating teeth} \\
 &= \Delta\delta + EL && \text{for same tooth}
 \end{aligned}
 \tag{5}$$

where:

- α = Profile modification
- SE = Spacing or profile error
- EL = Lead error along same tooth

5 Case Study

As an example for numerical treatment, a helical gear with an extreme rating of 1103 HP (827 KW) and 33,000 rpm speed is selected. This gear is considered the driver. A driven gear of larger face width is in contact with the driver. Gear data sheets for both gears are given in Table 1. Total normal force of 8980 Newtons is calculated based upon the given running conditions and gear geometry.

Table I: Gear Data

	Driver (Pinion)	Driven (Wheel)
Pitch Diameter, <i>mm</i>	59.0550	116.5352
Rim Diameter, <i>mm</i>	29.2100	101.6000
Root Diameter, <i>mm</i>	55.0672	112.1664
Effective Outside Diameter, <i>mm</i>	61.8490	119.0498
Form Diameter, <i>mm</i>	56.8859	114.1150
Fillet Radius, <i>mm</i>	0.4699	0.4597
Diameter at HPSTC, <i>mm</i>	60.5716	117.8573
Face Width, <i>mm</i>	29.9999	45.0088
Diameter at LPSTC, <i>mm</i>	57.8315	115.1384
Number of teeth	37	73
Module, <i>mm</i>		1.5961
Transverse Circular Tooth <i>th.</i> , <i>mm</i>	2.3063	2.1234
Helix Angle ψ , degrees		20
Transverse Pressure Angle ϕ_p , degrees		25

The angle between the contact line and the helix tangent ω is given by Baxer [8] as:

$$\sin \omega = \sin \psi \times \sin \phi_t \quad (6)$$

which upon substitution from the gear data sheet yields $\omega = 8.311$ degrees. Transverse contact ratio of 1.29 and face contact ratio of 2.18 are calculated from gear geometry. Therefore, a total contact ratio of 3.47 is expected which means that the number of contacting teeth vary between 3 and 4 during action. An instant when 4 teeth are in contact is selected for this study. Figure (4) shows a schematic drawing of the teeth from the form diameter up to the effective outside diameter OD . The

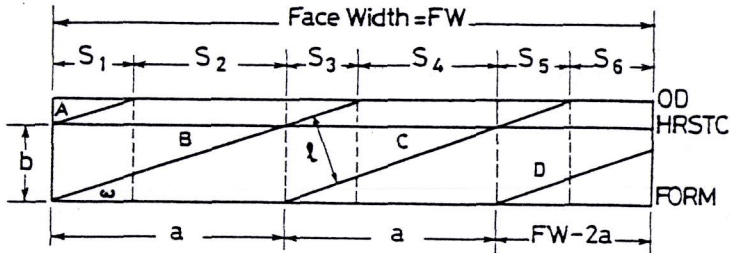


Figure (4) Tooth Slicing

diameter at the Highest Point of Single Tooth Contact (*HPSTC*) is also indicated and it is assumed that the first contact line *A* commences from there as shown in the figure. The rest of contact lines (*B*, *C* and *D*) are determined accordingly, so as parameters a , b , and ℓ .

For convenience, the gear was then sliced into sections $s_1, s_2, s_3, \dots, s_6$ as shown in the previous figure. Note that $s_1 = s_3 = s_5$ and $s_2 = s_4$. To further improve the model, each slice of the six slices shown in the figure was subdivided to four equal sections. The result is given in Figure (5). The stiffnesses of all segments modelling the entire helical gear as well as the load transmitted by each segment were then determined

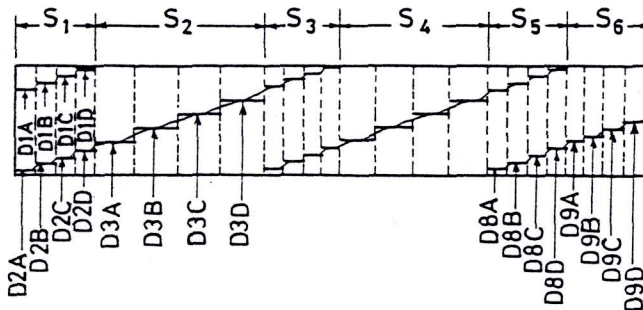


Figure (5) Model Improvement

using the above mentioned procedure. Lead and spacing errors were also considered and the distribution of loads along lines of contact was determined accordingly.

6 Results and Discussions

6.1 Lead Error Effect

To demonstrate the capability of the model in handling lead error effect, tooth *B* was assigned several error values up to 0.0254 mm, while other contacting teeth were kept error free. Load distribution in such cases is plotted graphically in Figure (6).

It is clear that such error increases the maximum transmitted load on tooth *B* from 498 Newtons, at zero error, to the values indicated in the figure. Lead error effect on adjacent tooth *A* was found to increase as well; while that on teeth *C* and *D* decreased in order to keep the total transmitted loads by contacting teeth constant; irrespective of individual loads. It is also clear that tooth *B* transmits the maximum load among all contacting teeth at this instant of time.

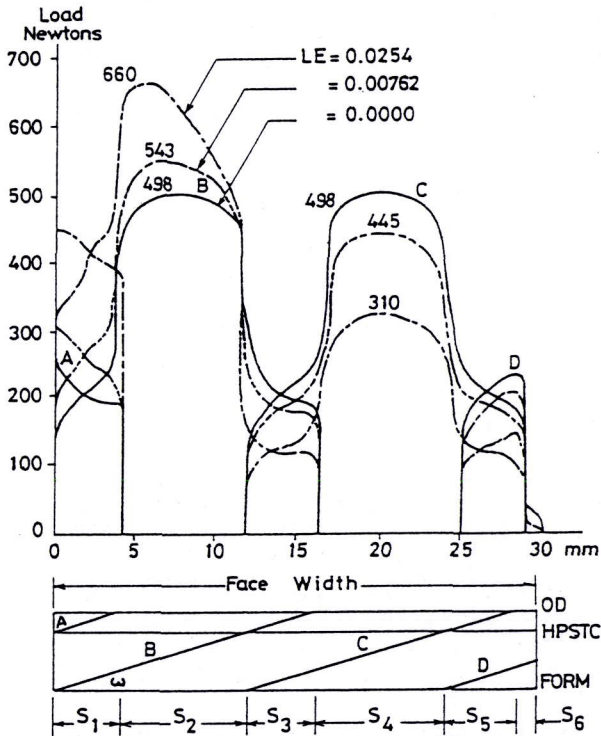


Figure (6) Lead Error Effect on Load Distribution

6.2 Spacing Error Effect

In order to investigate the effect of tooth spacing error on load distribution, tooth *B* was assigned several values of spacing error up to a value of 0.02286 mm while other contacting teeth were kept error free. Other forms of profile derivation (e.g. lead error, tip/root modification) were set equal to zero. Load distribution along each tooth contact line is plotted in Figure (7).

The maximum transmitted load was found to increase with the increase of spacing error as shown in the figure. Tooth *B* was found to transmit the maximum load in this case as well. Transmitted load on adjacent tooth *A* was found to increase with increasing spacing error on tooth *B*; while that for teeth *C* and *D* were found to decrease under same condition. Nevertheless, the total sum of transmitted loads by all teeth in actions was constant in all cases presented in the figure.

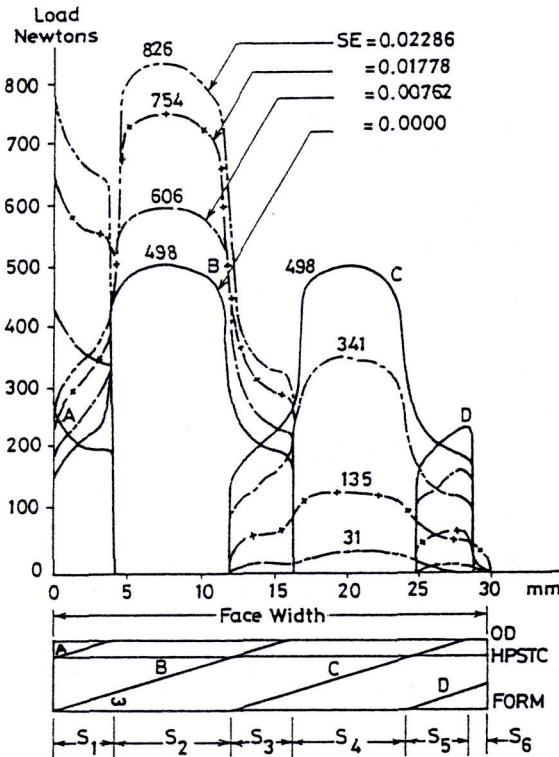


Figure (7) Spacing Error Effect on Load Distribution

7 Experimental Verification

The criterion outlined in this study was verified using experimental results carried out by Oda and Koide [9]. The main dimensions of the driving and driven gears are normal module = 6, normal pressure angle = 20° , helix angle = 20° , number of teeth = 36/36, face width = 55.11 mm. Total circumferential (tangential) load = 13.5 KN.

Tensile root stress wave forms produced in the fillet due to load transmission were measured using strain gauges located in the fillet at several positions along the face

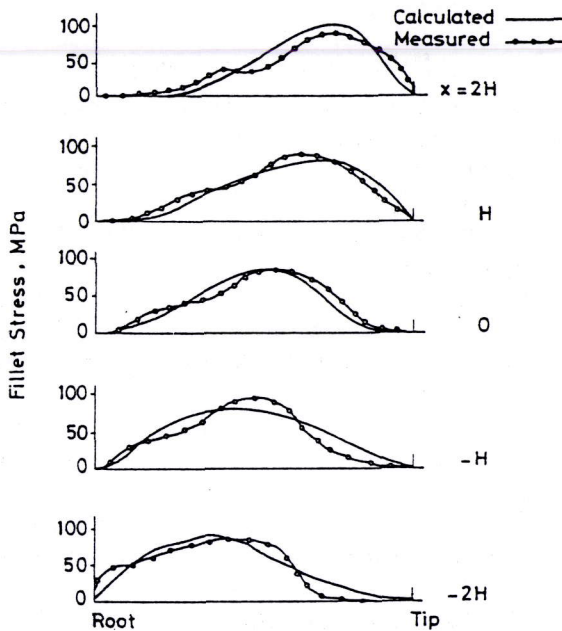


Figure (8) Comparison of Measured Fillet Stresses With Calculated Ones

width. The results are shown in Figure (8), where the station at $H = 0$ corresponds to the middle of the face width and the entire face width was made equal to $4H$.

Load distributions along contact lines were determined from the procedure given in this study; and corresponding tooth tensile fillet stress waveforms were determined using Aida and Terauchi formula [10], and then compared with the measured stresses. The calculated root stress waveforms agree fairly well with measured ones as shown in the figure. Thus the validity of the procedure presented in this study for calculating load distribution along contact lines for helical gears is considered to be fairly high.

8 Conclusion

The procedure presented in this study is of great help in determining load distribution and sharing on contact lines of helical teeth. Any forms of tooth profile deviation may be studied to its beneficial and non beneficial effect on the load distribution. In particular, the method described allows to analyze the influence of any given amount of tooth profile correction and to arrive at the determination of the optimum tooth profile correction of helical gears. Also it should be checked that the tooth profile correction is sufficient to compensate the adverse effect of tooth errors, particularly lead and spacing errors.

References

1. Neriya, S.V., Bhat, R. B., and Sankar, T. S., (1988), "On the Dynamic Response of a Helical Geared System Subjected to a Static Transmission Error in the Form of Deterministic and Filtered White Noise Inputs", *ASME Journal of Vibration, Acoustics, Stress, and Reliability in Design*, Vol. 110, pp. 501-506.
2. Livitin, F. L., Zhang, Y., et al., (1992), "Computerized Inspection of Real Surfaces and Minimization of their Deviations", *Int. J. Mach. Tools Manufact.*, Vol. 32, No. 1/2, pp.141-145.
3. Nakada, T., and Utagawa, M., (1956), "The Dynamic Loads on Gear Caused by the Varying Elasticity of the Mating Teeth", *Proceedings of the 6th Japanese National Congress for Applied Mechanics*, pp. 43, Japanese Society of Mechanical Engineers (JSME).
4. Kasuba, R., and Evans, J., (1981), "An Extended Model for Determining Dynamic Loads in Spur Gearing", *ASME Journal of Mechanical Design*, Vol. 103, pp. 398-409.
5. Elkholy, A. H., (1985), "Tooth Load Sharing in High Contact Ratio Spur Gears", *ASME Journal of Mechanisms, Transmissions, and Automation in Design*, Vol. 107, pp. 11-16.
6. Vijayakar, S. M., Sarkar, B., and Houser, D. R., (1987), "Gear Tooth Profile Determination from Arbitrary Rack Geometry", *AGMA paper 87 FTM4*.
7. Ueno, T., Ariura, Y., Kubo, A., and Nakanishi, T., (1984), "Effects of Tooth Form on Stresses in Helical Gears", *Bull. Japanese Society of Mechanical Engineers*, Vol. 27, No.233, pp. 2545-2552.
8. Baxer, M. L., (1962), "Gear Handbook, Chapter 1", Edited by Dudley, D. W., McGraw-Hill Book Co., First Edition, pp. 1.10-1.12.
9. Oda, S. and Koide, T., (1984), "Effects of Addendum Modification on Bending Fatigue Strength of Helical Gears", *Bulletin of the Japanese Society of Mechanical Engineers*, Vol. 27, No. 232, pp. 2272-2278.
10. Aida, T., and Terauchi, Y., (1962), "On the Bending Stress of a Spur Gear", *Bulletin of the Japanese Society of Mechanical Engineers*, Vol. 5, No. 17, pp. 161-179.